American Mineralogist, Volume 67, pages 494–509, 1982

Chemical models for lithium aluminosilicate stabilities in pegmatites and granites

DAVID LONDON[1] AND DONALD M. BURT

Department of Geology
Arizona State University
Tempe, Arizona 85281

Abstract

The primary lithium aluminosilicates in pegmatites are spodumene (α-$LiAlSi_2O_6$) and petalite ($LiAlSi_4O_{10}$). These minerals are frequently replaced by fine-grained assemblages of eucryptite (α-$LiAlSiO_4$), albite, micas, and clay minerals as a result of subsolidus cation exchange reactions with residual pegmatitic fluids.

All three of the lithium aluminosilicates may be converted to albite in quartz-saturated, Na-rich environments, but in quartz-undersaturated environments (as within large single crystals of spodumene), the replacement assemblage eucryptite + albite is stable to high values of the exchange potential $\mu_{NaLi_{-1}}$. The stability of the primary pegmatite assemblage quartz + albite + spodumene (or petalite) + amblygonite-montebrasite + lithiophilite means that lithiophilite or amblygonite-montebrasite cannot be altered to natrophilite ($NaMnPO_4$) or lacroixite ($NaAlPO_4F$), respectively, until Na–Li exchange has locally converted all of the lithium aluminosilicates to albite. Of the three lithium aluminosilicates, eucryptite is the most susceptible to replacement by muscovite, but spodumene also may be converted directly to mica ("killinite"). In acidic fluids with a high capacity to hydrolyze solid phases and leach alkali cations, the lithium aluminosilicates may be altered to (or become unstable relative to) kaolinite, cookeite, muscovite, lepidolite, and topaz. The common late-stage assemblage topaz + lepidolite + quartz forms in KF- and HF-rich environments outside of the lithium aluminosilicate stability region. All of the lithium aluminosilicates are unstable relative to amblygonite (or montebrasite) + quartz in P- and F-rich environments, but spodumene is stable to higher activities of these acidic volatiles than are eucryptite and petalite.

Introduction

In an accompanying paper (London and Burt, 1982) we propose several P–T diagrams involving the lithium aluminosilicates eucryptite (α-$LiAlSiO_4$), spodumene (α-$LiAlSi_2O_6$), beta-spodumene (β-$LiAlSi_2O_6$), petalite ($LiAlSi_4O_{10}$), and quartz in the binary system $LiAlSiO_4$–SiO_2. These phase diagrams offer explanations for (1) the absence of beta-spodumene in nature, (2) the occurrence of spodumene and petalite as the only primary lithium aluminosilicates in pegmatites, and (3) the isochemical replacements of petalite by spodumene + quartz, and of both petalite and spodumene by eucryptite + quartz, as reported from numerous localities. In particular, the proposed phase diagrams account for the stable assemblage eucryptite + quartz under subsolidus conditions of relatively low P and T.

In this paper, we evaluate lithium aluminosilicate stabilities in response to changing physico-chemical conditions by considering the effects of added components in the melt or aqueous fluid (as opposed to components in crystalline solid solutions). This treatment explains most aspects of the metasomatic replacement of lithium aluminosilicates (described below) and further defines the magmatic and post-magmatic conditions under which eucryptite, spodumene, and petalite may or may not form in pegmatites and lithium-rich granites. The phases to be considered are listed in Table 1.

Metasomatic replacement

Primary spodumene and petalite frequently exhibit partial to complete alteration to a variety of fine-grained mineral assemblages. Replacements of

[1]Present address: Geophysical Laboratory, 2801 Upton Street, N.W. Washington, D.C. 20008.

0003–004X/82/0506–0494$02.00

petalite by albite, micas, or clay minerals have been reported from numerous localities (*e.g.*, Quensel, 1937; McLaughlin, 1940; Nel, 1946; Saito *et al.*, 1950; Ginzburg and Gushchina, 1954; Rossovskii and Klochova, 1965). Metasomatically altered spodumene also is extremely common, as detailed in Table 2. The most frequently observed replacement assemblages are aggregates of albite, eucryptite + albite, mica (muscovite or lepidolite) + albite, and pure mica (Li-muscovite or lepidolite). These replacements are fine-grained and pseudomorphic in nature and appear to result from subsolidus reactions between spodumene (or petalite) and residual pegmatitic fluids.

The observations of Brush and Dana (1880) on the alteration of spodumene from Branchville, Connecticut, plus our own studies of specimens from Branchville, from Center Strafford, New Hampshire, and from the White Picacho district, Arizona (Burt *et al.*, 1977; London, 1979), show a similar sequence of replacement assemblages in spodumene. At these localities, spodumene in contact with primary quartz or quartz + albite commonly displays a reaction rim of pure albite, whereas the interiors of spodumene crystals are replaced to varying degrees by a fine-grained, fibrous intergrowth of eucryptite + albite (Fig. 1). This initial replacement is cleavage-controlled and results in bilaterally symmetrical veinlets of fibrous eucryptite + albite whose long fiber axes are oriented perpendicular to the {110} cleavage in the host spodumene (Fig. 1). Preliminary studies by electron diffraction and microscopy, however, indicate that neither albite nor eucryptite shows a preferred crystallographic orientation with respect to spodumene. The eucryptite + albite intergrowths commonly coarsen toward the centers of veinlets and display a vermiform or graphic texture (Fig. 1). In many samples, eucryptite near veinlet centers and spodumene crystal borders has been altered to muscovite or lepidolite (Fig. 1), resulting in the intergrowth of mica (usually muscovite) + albite called "cymatolite" by Brush and Dana (1880). Finally, remnant spodumene and secondary albite have been replaced by mica (lithian muscovite or lepidolite), producing soft, waxy pseudomorphs of nearly pure mica after spodumene (referred to as "killinite" by Julien, 1879). At these and other localities, spodumene also appears to have been converted directly to albite, mica + albite or pure mica (Table 2), but the alteration sequence described above and depicted schematically in Figure 2 appears to represent the most complete history of metasomatic alteration of spodumene in pegmatites.

The sequence of alteration assemblages described above suggests that initial alteration of spodumene fundamentally involved sodium-for-lithium ion exchange (as evidenced by the formation of albite±eucryptite, followed by potassium + hydrogen metasomatism (resulting in the conversion of eucryptite, then spodumene and albite, to mica). Of the more common pegmatite minerals, spodumene appears to be especially responsive to these metasomatic processes. The striking mineralogical and textural similarities of these alteration assemblages at many localities imply that these replacement events are a common and important part of the subsolidus evolution of lithium pegmatites.

Table 1. Names and compositions of phases discussed in this paper

Phase	Abbreviation used	Composition
eucryptite	Ecr	α-$LiAlSiO_4$
spodumene	Spd	α-$LiAlSi_2O_6$
petalite	Pet	$LiAlSi_4O_{10}$
quartz	Qtz	SiO_2
beta spodumene	---	β-$LiAlSi_2O_6$
albite	Alb	$NaAlSi_3O_8$
K-feldspar	Ksp	$KAlSi_3O_8$
nepheline	Nph	$NaAlSiO_4$
muscovite	Mus	$KAl_3Si_3O_{10}(OH)_2$
paragonite	Par	$NaAl_3Si_3O_{10}(OH)_2$
lepidolite	Lpt	$K(Li,Al)_3(SiAl)_4O_{10}(F,OH)_2$
polylithionite	---	$KLi_2AlSi_4O_{10}(F,OH)_2$
cookeite	---	$LiAl_4(AlSi_3)O_{10}(OH)_8$
kaolinite	Kao	$Al_2Si_2O_5(OH)_4$
topaz	---	$Al_2SiO_4(F,OH)_2$
amblygonite	Amb	$LiAlPO_4F$
lacroixite	Lac	$NaAlPO_4F$
montebrasite	---	$LiAlPO_4(OH)$
natromontebrasite	---	$NaAlPO_4(OH)$
lithiophilite	---	$LiMnPO_4$
triphylite	---	$LiFePO_4$
natrophilite	---	$NaMnPO_4$
columbite	---	$(Mn,Fe)(Nb,Ta)_2O_6$
tantalite	---	$(Fe,Mn)(Ta,Nb)_2O_6$
microlite	---	$(Na,Ca)_2Ta_2O_6(O,OH,F)$
pyrochlore	---	$(Na,Ca)_2Nb_2O_6(O,OH,F)$
cassiterite	---	SnO_2

The influence of Na-for-Li exchange on lithium aluminosilicate stabilities

The formation of secondary albite by replacement (albitization) of pre-existing pegmatite is a well documented and important phenomenon in the hydrothermal stage in the history of many lithium pegmatites. Pseudomorphic albitization of spodumene as described above has been identified at many localities, some of which are listed in Table 2. An analogous replacement of quartz-spodumene pegmatite by coarse-grained masses of albite (cleavelandite) also occurs in highly differentiated lithium pegmatites. In the United States, such replacements are well exposed and documented from the Harding pegmatite, New Mexico (Jahns and Ewing, 1976, 1977; Chakoumakos, 1978a, 1978b), and can be observed in outcrops at the Branchville pegmatite, Connecticut (Brush and Dana, 1880; Shainin, 1946), and at the Black Mountain pegmatite near Rumford, Maine (Page *et al.*, 1953). Replacement units of coarse-grained albite have been recognized in most major pegmatite districts in the United States (*e.g.*, see Jahns, 1946, 1955; Cameron *et al.*, 1949) and in the Soviet Union (*e.g.*, Beus, 1960; Vlasov, 1961, 1964–66), and they are an integral

Table 2. Some reported occurrences of pseudomorphed spodumene

Locality	Assemblage(s)	Reference(s)
Black Hills, South Dakota, USA	1. Mus	Schwartz & Leonard, 1926
	2. Kao	Schwartz, 1937
	3. Ecr+Alb (tentative)	Jones, 1964
Black Mtn., Maine, USA	1. Mus+Alb	USNM* #108688
	2. Alb	
Branchville, Connecticut, USA	1. Alb	Brush and Dana, 1880
	2. Ecr+Alb	
	3. Mus+Alb	
	4. Ksp+Alb	
	5. Mus	
Center Strafford, New Hampshire, USA	1. Ecr+Alb	Mrose, 1953
	2. Mus+Alb	Harvard Univ. #117231,117232
Dixon, New Mexico, USA	1. Alb	Mrose, 1953
	2. Li-mica	Jahns & Ewing, 1976, 1977
	3. Ecr+Qtz	Chakoumakos, 1978a, 1978b
	4. Ecr+Alb	
Gunnison County, Colorado USA	sericite	Hanley *et al.*, 1950
Huntington, Massachusetts, USA	1. Mus+Alb	Julien, 1879
	2. Mus	
Peg claims, Maine, USA	mica+Qtz (?)	Sundelius, 1963
Portland, Connecticut, USA	1. Alb	Jenks, 1935
	2. Mus	
White Picacho dist., Arizona USA	1. Alb	Burt *et al.*, 1977
	2. Ecr+Alb	London & Burt, 1979
	3. Mus+Alb	
	4. Mus	
Altyn Tau, USSR	1. Alb	Krygina, 1948
	2. Mus+Pet (?)	
Borborrema, Brazil	Ill**+Hal**	Rao, 1962
Bunsen mine, Korea	mica	Shibata, 1952
Itatiaia mine, Brazil	mica	USNM #122482
Katumba, Rwanda	Rb-mica	Varlamoff, 1960, 1961
Killiney, Ireland	mica	USNM #R4405
Kola Peninsula, USSR	1. Ecr+Alb	Sosedko & Gordienko, 1953
	2. Mus+Olg**	Sosedko, 1964
Lalín, Spain	Mus+Alb	Parga-Pondal & Cardoso, 1948
Myokenzan, Japan	1. Mus+Alb	Sakurai *et al.*, 1977
	2. Mus	
Ravensthorpe, Australia	mica	Graham, 1975
Siberia, USSR	Alb	Nazarova, 1961
Varutrask, Sweden	1. Mus+Alb	Quensel, 1938
	2. Hec** or Kao	

*USNM = U. S. National Museum, Smithsonian Institution, Washington, D. C.
**Hec = hectorite, Olg = oligoclase, Ill = illite, Hal = halloysite.

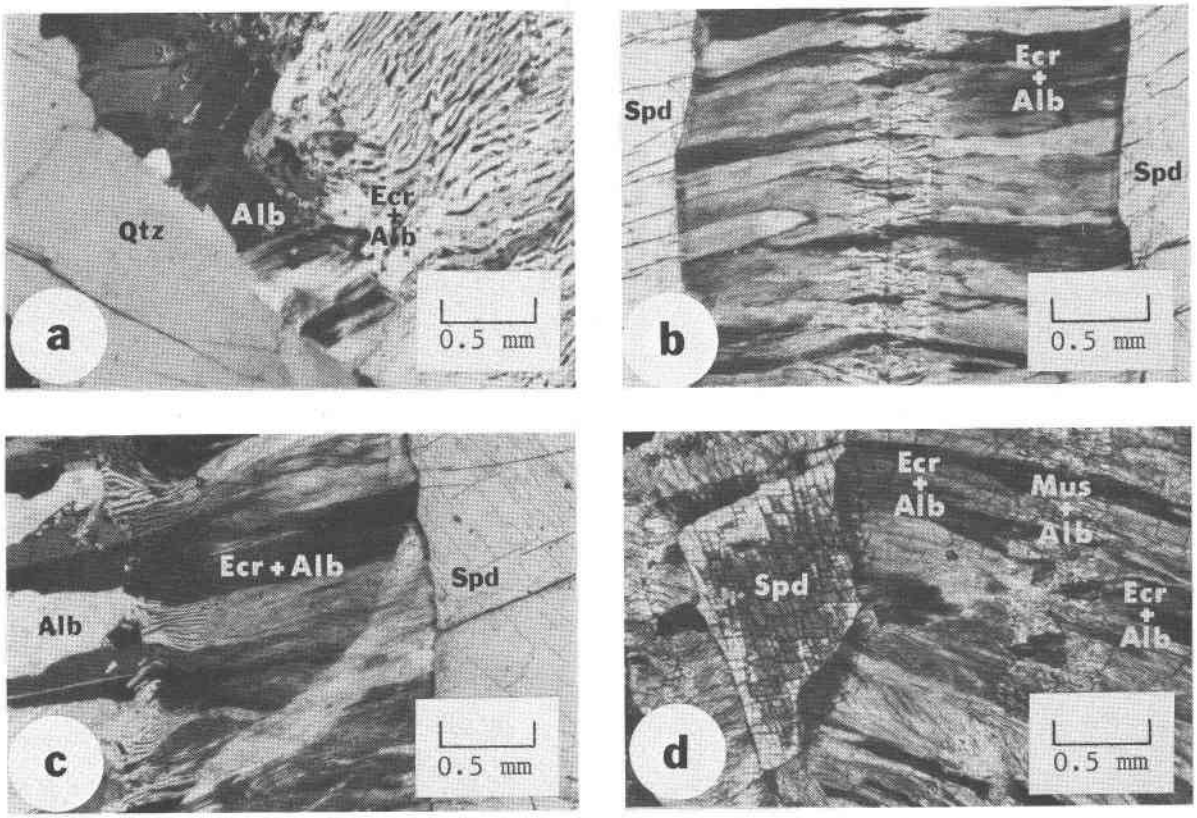

Fig. 1. Photomicrographs showing the pseudomorphic alteration of spodumene: (a) a thin reaction rim of albite (Alb) separating quartz (Qtz) from eucryptite (Ecr) + albite pseudomorph of spodumene from Branchville, Connecticut (Yale University specimen #C2684, courtesy of H. Winchell); (b) cleavage-controlled alteration of spodumene (Spd) to a fibrous intergrowth of eucryptite + albite from Branchville, Connecticut (Yale University specimen #C2648, courtesy of H. Winchell); (c) the vermiform or graphic texture of eucryptite + albite intergrowths after spodumene from the Buzzo pegmatite, Parker Mountain, near Center Strafford, New Hampshire (Harvard University specimen #117231, courtesy of C. A. Francis); (d) muscovite (Mus) + albite ("cymatolite") surrounding eucryptite + albite and relict spodumene from Branchville, Connecticut (Yale University specimen #C2670, courtesy of H. Winchell). The sections are viewed parallel to [001] in relict spodumene. All sections viewed in crossed polars.

part of most models for pegmatite crystallization (*e.g.*, Jahns and Burnham, 1969). Whether albitization of lithium aluminosilicates has produced coarse-grained cleavelandite or fine-grained pseudomorphs, it is presumably the result of sodium-for-lithium ion exchange (Na $\rightleftharpoons$ Li) between lithium aluminosilicates and a coexisting fluid.

The effects of Na $\rightleftharpoons$ Li on lithium aluminosilicate stabilities can be modelled in the system $LiAlSiO_4$–SiO_2–$NaLi_{-1}$, in which Na $\rightleftharpoons$ Li exchange is represented by the alkaline exchange operator $NaLi_{-1}$ (Burt, 1974). This system can be topologically reduced to the binary $MAlSiO_4$–SiO_2 (where M = Li or Na) by assuming that the chemical potential (μ) of $NaLi_{-1}$ is locally constant and may be externally controlled by the aqueous pegmatitic fluid, thus removing one degree of freedom from the solid-phase (rock) system under consideration. The chemical potential of the component $NaLi_{-1}$ might be considered $= \mu_{NaCl} - \mu_{LiCl} = \mu^{\circ}_{NaCl} - \mu^{\circ}_{LiCl} + RT\ln(a_{NaCl}/a_{LiCl})$. The assumption that the chemical potential of $NaLi_{-1}$ (and of several other components employed in subsequent diagrams) is fluid-controlled is based on observations from complex lithium pegmatites. Numerous secondary minerals (especially late-stage albite) occur at sharp metasomatic replacement fronts that are texturally and spatially similar to calc-silicate exoskarn replacement fronts in carbonate rocks (*cf.* Burt, 1977). The completeness of replacement seems to indicate that the solid phases undergoing alteration do not buffer individual cation activities (or cation exchange potentials) in the fluid on a gross scale. In the following models, we assume that crystal-fluid equilibri-

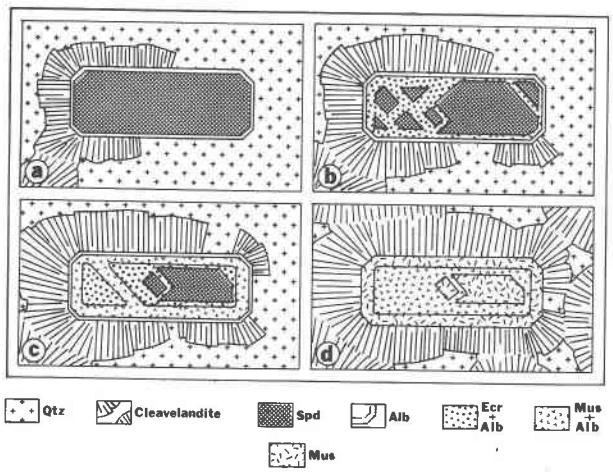

Fig. 2. Schematic depiction of the general alteration scheme for spodumene crystals embedded in quartz. The view of spodumene is down [001]. Replacement proceeds along crystal boundaries and {110} cleavage in spodumene. Coarse-grained albite (cleavelandite) radiates from spodumene borders; and the amount of cleavelandite increases as alteration proceeds. This sequence is typical of spodumene from Branchville, Connecticut, Center Strafford, New Hampshire, the White Picacho district, Arizona, and probably from numerous other localities.

um is attained locally (along crystal boundaries, cleavages, *etc.*), and that the chemical potentials of perfectly mobile components may be regarded as constant at this scale.

The compositional relations on the binary MAlSiO$_4$–SiO$_2$ are summarized in Figure 3; molar volume and entropy data for these phases are compiled in Table 3. The compositional data lead to nine reactions among these phases; seven of these reactions are listed in Table 4. The reactions are univariant lines that radiate from four possible (stable or metastable) invariant points on $P_s - \mu_{NaLi_{-1}}$ or $T - \mu_{NaLi_{-1}}$ diagrams. The slopes of these lines, listed in Table 4, are derived from the thermodynamic relations involving mobile components (Thompson, 1955; Korzhinskii, 1959):

$$d\Delta G = \Delta V_s dP_s - \Delta S_s dT + \sum_a^z \Delta \nu_i d\mu_i, \qquad (1)$$

in which V and S are extensive properties of the solid-phase reactants, P is isotropic lithostatic pressure, $\mu_a \cdots \mu_z$ are the chemical potentials of "perfectly mobile" components in the environment of the solid-phase system, and $\nu_a \cdots \nu_z$ are the stoichiometry coefficients of these components in a given reaction.

At equilibrium ($d\Delta G = 0$),

$$\left(\frac{\partial P_s}{\partial \mu_a}\right) T, \mu_b, \cdots, \mu_z = -\frac{\Delta \nu_a}{\Delta V_s} \qquad (2)$$

$$\left(\frac{\partial T}{\partial \mu_a}\right) P, \mu_b, \cdots, \mu_z = +\frac{\Delta \nu_a}{\Delta S_s} \qquad (3)$$

$$\left(\frac{\partial \mu_a}{\partial \mu_b}\right) P, T, \mu_c, \cdots, \mu_z = -\frac{\Delta \nu_b}{\Delta \nu_a} \qquad (4)$$

Equations (2), (3), and (4), respectively, and the data in Table 3 give the slopes of reaction lines on $\mu_a - P_s$, $\mu_a - T$, and $\mu_a - \mu_b$ diagrams such as will be used below.

On a schematic isothermal $P_s - \mu_{NaLi_{-1}}$ phase diagram (Fig. 4) drawn for relatively low temperatures, note that increasing $\mu_{NaLi_{-1}}$ (or increasing alkalinity of the fluid) leads to reactions that are terminal to all three lithium aluminosilicates under quartz-saturated conditions, but for quartz-absent compositions, eucryptite is stable to higher values of $\mu_{NaLi_{-1}}$ (upper right) than is either spodumene or petalite (until at much higher values of $\mu_{NaLi_{-1}}$, eucryptite would theoretically be converted to nepheline). At relatively high pressure within the spodumene + quartz stability field, increasing $\mu_{NaLi_{-1}}$ results first in the conversion of spodumene + quartz to albite via reaction (Ecr, Pet). With increasing $\mu_{NaLi_{-1}}$, spodumene itself becomes unstable, breaking down to eucryptite + albite via reaction (Qtz, Pet). Conversion of spodumene to eucryptite + albite can occur only in quartz-undersaturated environments (*e.g.*, within large spodumene crystals). Eucryptite is not stable in the

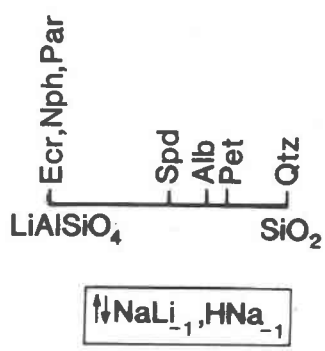

Fig. 3. Positions of phases on the binary composition coordinate MAlSiO$_4$–SiO$_2$ (M = H, Li, or Na) in the system LiAlSiO$_4$–SiO$_2$–NaLi$_{-1}$–HNa$_{-1}$. See Table 1 for phase abbreviations.

Table 3. Molar volume and entropy data on phases in the system $LiAlO_2$–SiO_2–$NaLi_{-1}$–PFO_2

Phases	V^o, joules/bar	S^o_{298}, joules/mole-K
Ecr	4.797(5)**	90(2)***
Spd	5.837(2)	129.30(80)
Bsp	7.825(4)	154.40(1.20)
Pet	12.840(5)†	232.200(2.092)††
Qtz	2.2688(1)	41.46(20)
Alb	10.007(13)	207.40(40)
Amb	4.758(10)†	---

*Data from Robie et al. (1978), except as follows:
**from Tien and Hummel (1964)
***calculated as explained by London and Burt (1982b)
†calculated from X-ray data (JCPDS file cards 14-90 and 22-1138)
††from Bennington et al. (1980)

presence of the common pegmatite assemblage quartz + albite + spodumene. Notice that ΔV_s for reactions (Ecr, Pet) and (Qtz, Pet) is relatively large (Table 4). Conversion of a small amount of spodumene to albite±eucryptite may effectively seal off fractures and inhibit the reaction by restricting fluid infiltration. This may account for the abundance of spodumene relicts within partial pseudomorphs.

There are two possible topologies for schematic isobaric $T - \mu_{NaLi_{-1}}$ phase diagrams in this system. These different topologies result from the fact that the slope of reaction (Alb, Pet) (Table 4), which is equivalent to reaction (Bsp, Pet) in Table 5 of London and Burt (1982), actually may be subhorizontal with a positive or negative slope in P–T space. The slope of this reaction becomes slightly negative if the entropy of eucryptite is only 2.2 joules/mole lower than the estimated value given in Table 3. This variation is roughly equal to the probable uncertainty for the estimated $S^\circ_{298.15}$ of eucryptite, and it is within the uncertainty of ΔS for reaction (Pet, Bsp) (London and Burt, 1982, Table 5), if uncertainties for individual phases are propagated. In both possible $T - \mu_{NaLi_{-1}}$ phase diagrams, as in the $P_s - \mu_{NaLi_{-1}}$ diagram (Fig. 7), increasing $\mu_{NaLi_{-1}}$ is terminal to petalite, spodumene, and eucryptite in quartz-saturated environments, but eucryptite is stable with albite to much higher values of $\mu_{NaLi_{-1}}$ under quartz-absent conditions. The assumption that the slope of reaction (Pet, Bsp) is positive in P–T space results in a topology in $T - \mu_{NaLi_{-1}}$ space that is compatible with Figure 4 and with natural occurrences. In agreement with observed assemblages, Figure 5, drawn for relatively low pressures, suggests that at arbitrary P, the assemblage spodumene + quartz is stable to higher values of $\mu_{NaLi_{-1}}$ than is eucryptite + quartz or petalite + quartz. For assemblages whose bulk compositions are less siliceous than albite (*i.e.*, for Si:Al < 3), eucryptite + albite is stable to high values of $\mu_{NaLi_{-1}}$. Notice also in Figures 4 and 5 that the isochemical breakdown of petalite or spodumene to eucryptite + quartz (London and Burt, 1982) occurs only at low values of P, T, and $\mu_{NaLi_{-1}}$.

Sodium-for-lithium exchange involving silicates and phosphates

Some additional aspects of Na ⇌ Li in pegmatites are illustrated by the apparent mineral compatibili-

Table 4. Some univariant reactions in the system $LiAlSiO_4$–SiO_2–$NaLi_{-1}$ (Figs. 4 and 5)

Phases absent	Reaction	ΔV_s	ΔS_s	$(\delta P/\delta \mu_{NaLi_{-1}})_T$	$(\delta \mu_{NaLi_{-1}}/\delta_T)_P$
(Ecr,Pet)	Spd + Qtz + $NaLi_{-1}$ = Alb	+1.90	+36.64	+0.5	-36.6
(Alb,Pet)	Spd = Ecr + Qtz	+1.23	+2.16	0.0	∞
(Qtz, Pet)	2Spd + $NaLi_{-1}$ = Ecr + Alb	+3.13	+38.80	+0.3	-38.8
(Spd. Pet)	Ecr + 2Qtz + $NaLi_{-1}$ = Alb	+0.67	+34.48	+1.5	-34.5
(Alb, Spd)	Ecr + 3Qtz = Pet	+1.23	+17.82	0.0	∞
(Ecr, Spd)	Pet + $NaLi_{-1}$ = Alb + Qtz	-0.56	+16.66	-1.8	-16.7
(Qtz, Spd)	Ecr + 2Pet + 3$NaLi_{-1}$ = 3Alb	-0.46	+67.80	-6.5	-22.6

ties in the quartz-saturated reciprocal quaternary system $LiAlO_2$–$LiAlPO_4F$–$LiMnPO_4$–$NaLi_{-1}$ (Fig. 6). This diagram shows as stable the assemblage quartz + albite + spodumene (or petalite or eucryptite) + amblygonite (or montebrasite) + lithiophilite (or triphylite). As noted above, increasing $\mu_{NaLi_{-1}}$ under quartz-saturated conditions results in the conversion of all three lithium aluminosilicates to albite. The stability of the assemblage quartz + albite + amblygonite-montebrasite + lithiophilite implies that the rare sodium phosphates lacroixite ($NaAlPO_4F$), natromontebrasite ($NaAlPO_4OH$) and natrophilite ($NaMnPO_4$) are incompatible with lithium aluminosilicates in the presence of quartz; thus the presence of lithium aluminosilicates + quartz precludes the formation of lacroixite, natromontebrasite or natrophilite by $Na \rightleftharpoons Li$ in ambylgonite-montebrasite or lithiophilite, respectively. Under quartz-saturated conditions, the local formation of sodium phosphates should not occur until all of the lithium aluminosilicates have been converted to albite (or otherwise destroyed). The degree of sodium metasomatism apparently varies with location in complex lithium pegmatites, and sodium metaso-

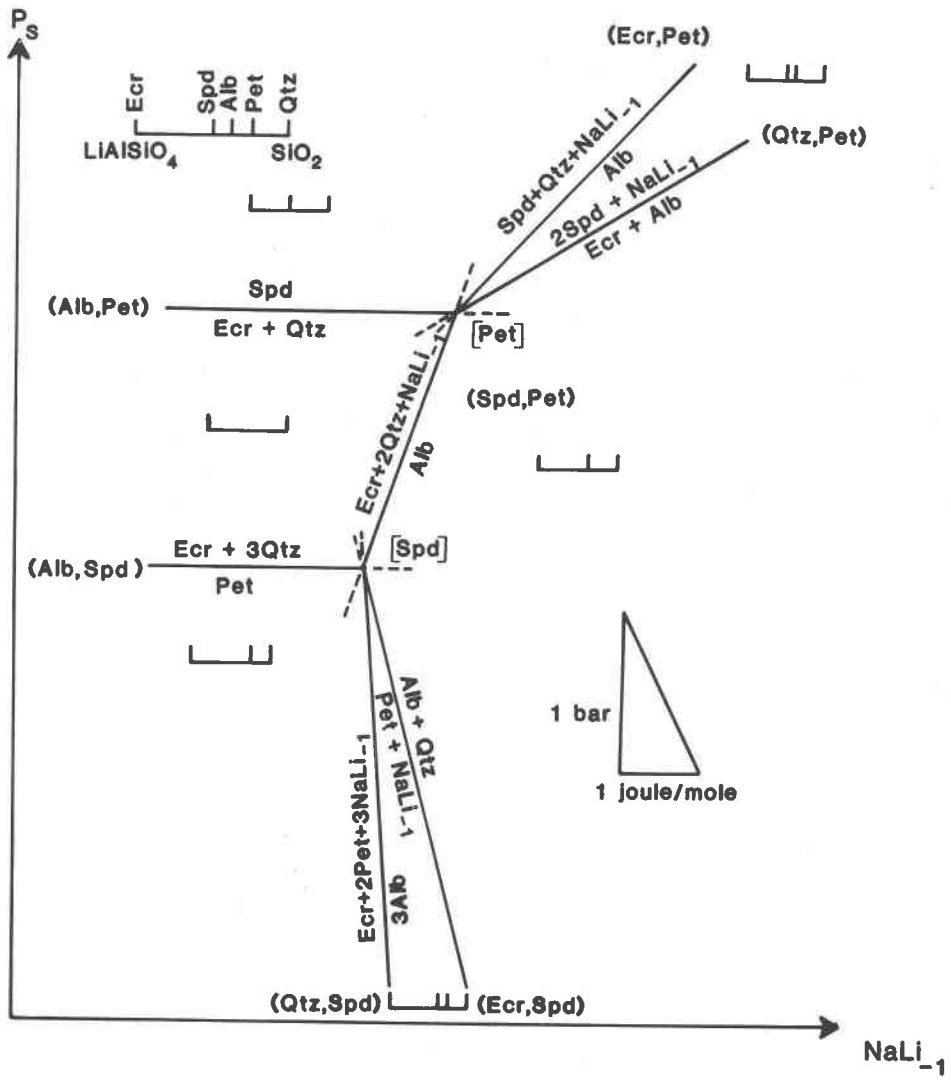

Fig. 4. Schematic isothermal P_s–$\mu_{NaLi_{-1}}$ phase diagram in the system $LiAlSiO_4$–SiO_2–$NaLi_{-1}$, constructed from reactions in Table 4 using data in Table 3 to determine slopes. Temperatures chosen are low enough that eucryptite + quartz is a stable assemblage. The topology of reactions around the invariant points [Ecr] and [Qtz] is not shown. The triangular scale marker in this and subsequent phase diagrams illustrates the relative slopes of reaction lines.

Table 5. Some univariant reactions in the system $LiAlSiO_4$–SiO_2–$NaLi_{-1}$–HNa_{-1} (Figs. 7 and 8)

Reactions	$(\delta\mu_{NaLi_{-1}}/\delta\mu_{SiO_2})_{P,T}{}^{\mu}{}_{HNa_{-1}}$	$(\delta\mu_{HNa_{-1}}/\delta\mu_{NaLi_{-1}})_{P,T}{}^{\mu}{}_{SiO_2}$	$(\delta\mu_{HNa_{-1}}/\delta\mu_{SiO_2})_{P,T}{}^{\mu}{}_{NaLi_{-1}}$
$Ecr + SiO_2 = Spd$	∞	---	∞
$Ecr + NaLi_{-1} = Nph$	0.0	∞	---
$Ecr + 2SiO_2 + NaLi_{-1} = Alb$	-2	∞	∞
$Spd + SiO_2 + NaLi_{-1} = Alb$	-1	∞	∞
$3Nph + 2HNa_{-1} = Par$	---	0.0	0.0
$3Ecr + 3NaLi_{-1} + 2HNa_{-1} = Par$	0.0	-3/2	0.0
$3Alb + 2HNa_{-1} = Par + 6SiO_2$	∞	0.0	+3
$3Spd + 3NaLi_{-1} + 2HNa_{-1} = Par + 3SiO_2$	+1	-3/2	+3/2

matism of lithium phosphates may occur where lithium aluminosilicates are absent or totally consumed, as in the formation of natrophilite at Branchville, Connecticut (Brush and Dana, 1880); and lacroixite at the spodumene-bearing Strickland pegmatite, Portland, Connecticut (Mrose, 1971).

Influence of $\mu_{NaLi_{-1}}$ on μ_{SiO_2} during albitization of spodumene

It is apparent from Figure 5 that along any isobaric cooling path within the divariant spodumene + quartz stability field, albitization of spodumene can be accomplished only by an increase in $\mu_{NaLi_{-1}}$ in the coexisting magma or aqueous fluid. Whether spodumene breaks down to albite via reaction (Ecr, Pet) or to eucryptite + albite via reaction (Qtz, Pet) depends on the presence or absence or quartz, and thus on μ_{SiO_2} (London and Burt, 1980). A schematic isobaric-isothermal $\mu_{NaLi_{-1}}$–μ_{SiO_2} phase diagram (Figure 7 and Table 5) in the system $LiAlSiO_4$–SiO_2–$NaLi_{-1}$ reveals that with increasing $\mu_{NaLi_{-1}}$, albitization of spodumene may take either of two paths. At subsolidus conditions, $\mu_{NaLi_{-1}}$ may increase along the spodumene-quartz univariant line until a ternary eutectoid involving spodumene, albite, and quartz is reached (point A in Figure 7). From point A, which is equivalent to the spodumene + albite + quartz ternary eutectic suggested by Stewart (1978), increasing $\mu_{NaLi_{-1}}$ under quartz-saturated conditions results in the consumption of spodumene and quartz to form (additional) albite. Where quartz is

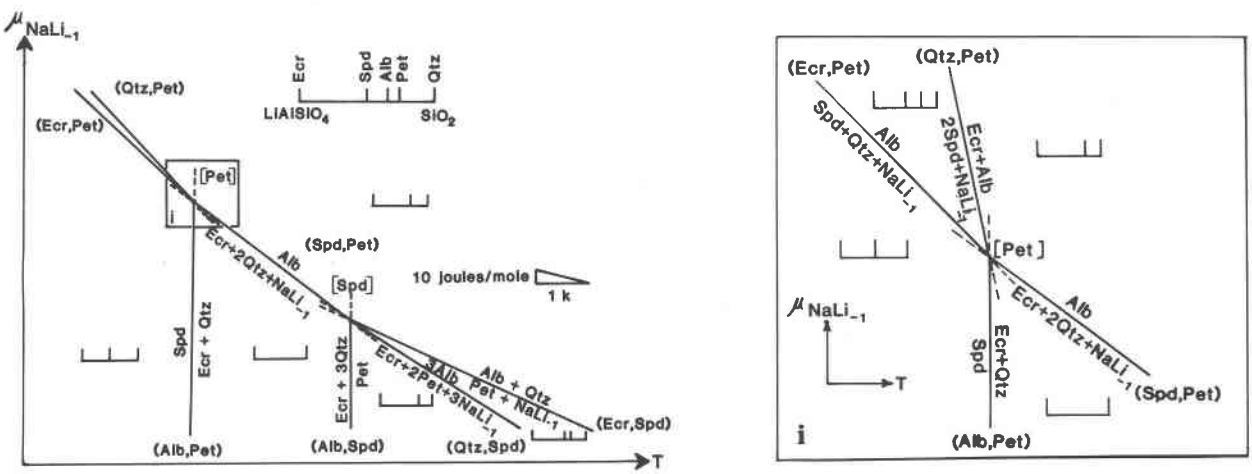

Fig. 5. Schematic isobaric $T - \mu_{NaLi_{-1}}$ phase diagram in the system $LiAlSiO_4$–SiO_2NaLi_{-1}, constructed for relatively low pressures and temperatures from reactions listed in Table 4, using data in Table 3 to determine slopes. The topology of univariant reactions at point [Pet] has been expanded in *i* (insert) to show the stable assemblages.

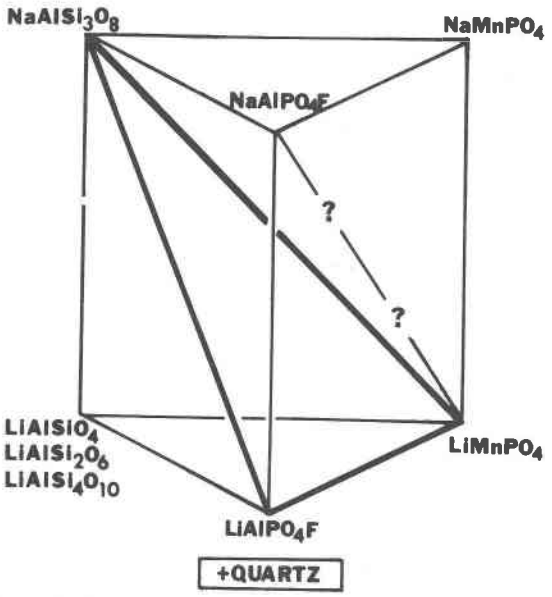

Fig. 6. Apparent mineral compatibilities in the quartz-saturated reciprocal quaternary system $LiAlO_2$–$LiAlPO_4F$–$LiMnPO_4$–$NaLi_{-1}$. Assuming that albite + amblygonite + lithiophilite + quartz is a stable assemblage in lithium pegmatites implies that the lithium aluminosilicates are incompatible with natrophilite or lacroixite in the presence of quartz.

absent (*i.e.*, within spodumene crystals), increasing $\mu_{NaLi_{-1}}$ again results in conversion of spodumene to albite, but with a drastic reduction in μ_{SiO_2}, as silica in solution is consumed by the albite-forming reaction (Table 5). Under equilibrium conditions, the reaction of spodumene to albite with increasing $\mu_{NaLi_{-1}}$ produces a steady decrease in μ_{SiO_2} (along with path *AB*, Figure 7) until a ternary eutectoid of eucryptite–albite–spodumene is reached (at point *B*, Figure 7). At this point, spodumene is converted to eucryptite + albite. Increasing $\mu_{NaLi_{-1}}$ from point *B* would produce a further reduction in μ_{SiO_2} as eucryptite reacts to form albite via reaction (Spd, Pet), and under extremely alkaline conditions of high $\mu_{NaLi_{-1}}$ and low μ_{SiO_2}, eucryptite would be converted, theoretically, to nepheline. Natural mineral assemblages, however, indicate that the highly alkaline conditions necessary to convert eucryptite to nepheline are not attained in late-stage subsolidus environments in pegmatites, and that micas are formed instead.

Conversion of lithium aluminosilicates to micas

All three lithium aluminosilicates, but especially eucryptite and spodumene, are susceptible to replacement by micas. Eucryptite is most vulnerable to this alteration (London and Burt, 1979); where eucryptite, spodumene, and albite coexist, eucryptite invariably is the first of these three minerals to be replaced by mica (Figs. 1 and 2). This fact, together with the observation that eucryptite never is replaced by nepheline, implies that the alkali cation leaching capacity and a_{H_2O} of late-stage pegmatitic fluids is (or becomes) sufficiently great that eucryptite is converted to mica, rather than albite or nepheline as implied by Figure 7 in quartz-undersaturated environments.

The effects of increasing cation leaching capacity of the fluid on lithium aluminosilicate stabilities can be modelled schematically by isobaric–isothermal phase diagrams in the system $LiAlSiO_4$–SiO_2–$NaLi_{-1}$–HNa_{-1}, involving the phases eucryptite, spodumene, albite, quartz, and paragonite (although natural micas in this association are muscovites or lepidolites). In this simplified model system, the chemical potential of the acidic cation exchange operator HNa_{-1} monitors the cation leaching capacity of the fluid, or the tendency for solids to undergo hydrolysis with a loss of alkali cations to the fluid.

Figure 8, which is constructed from the reactions listed in Table 5, reveals that with increasing $\mu_{HNa_{-1}}$, eucryptite, spodumene, and albite may be converted directly to mica, and at high values of $\mu_{HNa_{-1}}$, only mica + quartz is stable. Albitization of spodumene at low $\mu_{HNa_{-1}}$ may follow path *AB* in

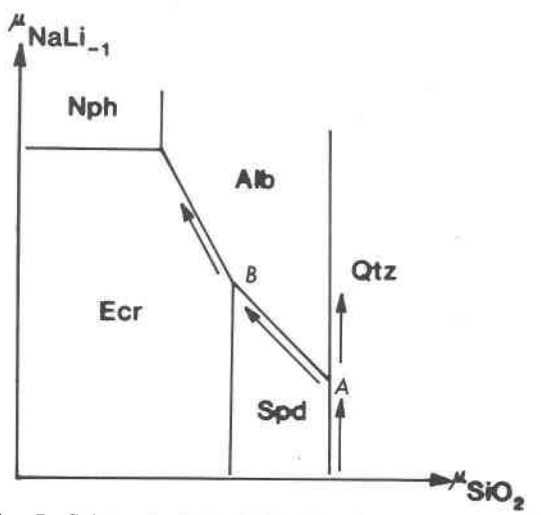

Fig. 7. Schematic isobaric–isothermal $\mu_{NaLi_{-1}}$–μ_{SiO_2} phase diagram in the system $LiAlSiO_4$–SiO_2–$NaLi_{-1}$, constructed from reactions in Table 5 at temperatures sufficiently low that petalite is unstable. Arrows and italicized letters indicate possible reaction paths, as explained in the text.

Figure 8, as spodumene is altered first to albite, and at somewhat lower μ_{SiO_2}, to eucryptite + albite. Increasing $\mu_{HNa_{-1}}$ along path *BC* in Figure 8 produces no observable change in the system until point *C* is attained, whereupon eucryptite reacts to form paragonite (Table 5). In natural environments, eucryptite is converted to muscovite by the reaction

$$\underset{\text{eucryptite}}{3LiAlSiO_4} + 2H^+ + K^+ = \underset{\text{muscovite}}{KAl_3Si_3O_{10}(OH)_2} + 3\,Li^+$$

Conversion of eucryptite to mica probably is facilitated by the fact that the Al:Si ratios are the same in both phases and that ΔV_s is small, so that reaction may be accomplished simply by exchange of cations. At a value of $\mu_{HNa_{-1}}$ slightly above *C'* (Fig. 8), the solid phase assemblage consists of mica, albite, and relict spodumene, but increasing $\mu_{HNa_{-1}}$ along path *CD* (Fig. 8) results in the direct and simultaneous conversion of albite and relict spodumene to mica. If albitization of spodumene occurs at values of $\mu_{HNa_{-1}}$ greater than *C'* (Fig. 8), eucryptite (+ albite) will not be formed, and partially albitized spodumene will break down directly to mica + albite ("cymatolite"). In Table 5, note that although the reaction of spodumene and of albite to mica liberates silica, quartz will not be formed if prior albitization locally has lowered μ_{SiO_2} below the quartz-saturation value (*e.g.*, to some value along the path *AB* (Fig. 7 and 8). This explanation, and the fact that mica-pseudomorphed spodumene typically is embedded in secondary cleavelandite (Fig. 2), may account for the absence of quartz in "killinite" from most localities (*e.g.*, Graham, 1975).

This model, and the reaction path described above for Figure 8, explains the occurrences of albite-rimmed spodumene crystals whose interiors are replaced successively by eucryptite + albite, mica + albite ("cymatolite"), and finally by pure mica ("killinite"). Although this model has been proposed to account for the fine-grained pseudomorphic replacement of spodumene described from many localities (Table 2), it may be applicable also to the sequential development of albite, albite + lepidolite, and lepidolite replacement complexes in highly differentiated lithium pegmatites. Differences in temperature of crystallization, degree of fracturing, and the volume of aqueous pegmatitic fluid may be responsible for determining whether the replacement of spodumene-bearing pegmatite is relatively widespread and coarse-grained or fine-grained and pseudomorphic. In both alteration schemes, the replacement of spodumene reflects alteration first by alkaline fluids (resulting in albitization), followed by increasingly acidic fluids (producing mica + quartz assemblages characteristic of weak greisenization).

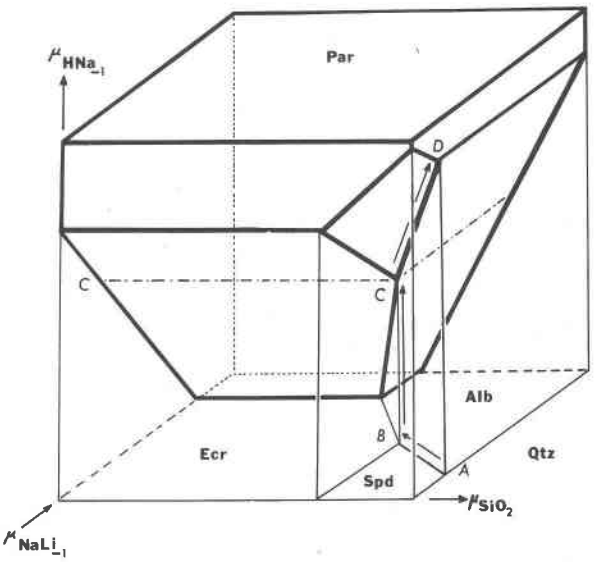

Fig. 8. Schematic isobaric–isothermal $\mu_{NaLi_{-1}}$–μ_{SiO_2}–$\mu_{HNa_{-1}}$ phase diagram constructed from reactions in Table 5. Heavy solid lines delineate the stability field of paragonite. Arrows and italicized letters indicate possible reaction paths, as explained in the text.

Lithium aluminosilicate stabilities in phosphorus- and fluorine-rich environments

The effects of increasing activities of the acidic volatiles P and F on lithium aluminosilicate stabilities can be modelled schematically in the system $LiAlO_2$–SiO_2–PFO_2, which contains the phases eucryptite, spodumene, petalite, amblygonite, and quartz (Fig. 9). Assuming that μ_{PFO_2} (= $\mu_{H_3PO_4}$ + μ_{HF} − $2\mu_{H_2O}$ = $1/2\mu_{P_2O_5}$ + $1/2\mu_{F_2O_{-1}}$) is constant (and in this case, probably externally controlled by the aqueous fluid phase) topologically reduces the system to two components. Based on the univariant reactions listed in Table 6, a schematic isothermal P_s − μ_{PFO_2} phase diagram depicting the topology of possible reactions at invariant points containing amblygonite and quartz (Fig. 10) illustrates that with increasing μ_{PFO_2}, all lithium aluminosilicates are converted to amblygonite + quartz. Notice, though, that spodumene is stable to higher values of μ_{PFO_2} than is either eucryptite or petalite. In Figure

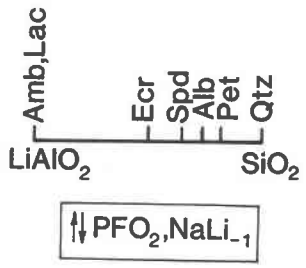

Fig. 9. Position of phases on the binary $LiAlO_2$–SiO_2 in the system $LiAlO_2$–SiO_2–PFO_2–$NaLi_{-1}$. See Table 1 for the abbreviations of phase names.

10, note that eucryptite breaks down with increasing μ_{PFO_2} to amblygonite + spodumene via reaction (Qtz, Pet) (Table 6), and thus the very common lithium pegmatite assemblage spodumene + amblygonite + quartz precludes the stable existence of eucryptite (or petalite).

Lithium aluminosilicate–montebrasite stability reactions are presumably analogous to those involving amblygonite, except that lithium aluminosilicates are converted to montebrasite + quartz at high $\mu_{H_3PO_4}$ (*i.e.*, under aqueous P-rich and F-poor conditions). Loh and Wise (1976) determined experimentally that at 500°C and 2 kbars fluid pressure, amblygonite-montebrasite at the compositional boundary (6.5 wt% F) is in equilibrium with a vapor in which log $f_{HF} < -3.0$. For comparison, this value is over three orders of magnitude lower than log f_{HF} at the lower stability limit of trilithionite (lepidolite) + quartz at the same P and T (Munoz, 1971).

Lithium aluminosilicate stabilities in alkaline *versus* acidic environments

The effects of increasing acidity (represented by PFO_2) *versus* increasing alkalinity (represented by $NaLi_{-1}$) of a magma or fluid on lithium aluminosilicate stabilities can be evaluated schematically in an isobaric–isothermal $\mu_{PFO_2} - \mu_{NaLi_{-1}}$ phase diagram in the system $LiAlO_2$–SiO_2–PFO_2–$NaLi_{-1}$ (Fig. 11). One possible diagram, which is constructed for temperatures sufficiently low that petalite is unstable, includes the phases eucryptite, spodumene, albite, amblygonite, lacroixite, and quartz (Figure 11 and Table 7). Assuming that μ_{PFO_2} and $\mu_{NaLi_{-1}}$ are constant makes it possible to project onto the binary $LiAlO_2$–SiO_2 (Fig. 9). Although this is an (n+4)-phase multisystem that might contain as many as fifteen stable or metastable invariant points, only four stable invariant points are shown in Figure 11. This simplification results from the assumed incompatibility of eucryptite with quartz in the presence of spodumene, and of spodumene with lacroixite. The lefthand side of Figure 11 (along the μ_{PFO_2} axis) shows that spodumene is stable to higher activities of the acidic volatiles P and F than is eucryptite (*cf.* the high-pressure portion of Figure 10). Conversely, eucryptite is stable to higher values of Na $\rightleftharpoons$ Li along the bottom ($\mu_{NaLi_{-1}}$) axis than is spodumene. With increasing values of both μ_{PFO_2} and $\mu_{NaLi_{-1}}$ (*i.e.*, in the presence of fluids rich in sodium salts of phosphorus and fluorine), both lithium aluminosilicates become unstable relative to amblygonite + albite at point [Qtz, Lac]. Lacroixite becomes stable (replacing amblygonite) only at very high values of $\mu_{NaLi_{-1}}$. Nepheline would replace eucryptite at still higher values of $\mu_{NaLi_{-1}}$ (not shown on Figure 11).

Lithium aluminosilicate stabilities in saline KF *versus* acidic HF environments could be evaluated in the model system $LiAlO_2$-SiO_2–KF–LiF–HF–H_2O. Graphical depiction of stability relations in this system is very difficult due to the large number of components and possible phases involved. Nevertheless, some aspects of lithium aluminosilicate stabilities in H-, K-, and F-rich environments can be tentatively explained. In relatively acidic H-rich fluids, Li may be leached from the lithium aluminosilicates to form kaolinite, or at higher values of μ_{LiF}, cookeite. In acidic HF-rich environments, the lithium aluminosilicates (and all other phases) become unstable relative to topaz + quartz. Lithium aluminosilicates are readily altered to muscovite by mildly acidic K- and H-rich fluids. In saline KF-rich conditions, the lithium aluminosilicates may be replaced by K-feldspar (at low values of μ_{LiF}) or by polylithionite (at relatively high values of μ_{LiF}).

Table 6. Univariant reactions in the system $LiAlO_2$–SiO_2–PFO_2 (Fig. 10)

Phases absent	Reactions	ΔV_s	$(\delta P/\delta \mu_{PFO_2})_T$
(Amb, Pet)	Spd = Ecr + Qtz	+1.23	0.0
(Spd, Pet)	Ecr + PFO_2 = Amb + Qtz	+2.23	+0.4
(Ecr, Pet)	Spd + PFO_2 = Amb + 2Qtz	+3.46	+0.3
(Qtz, Pet)	2Ecr + PFO_2 = Spd + Amb	+1.01	+1.0
(Amb, Spd)	Ecr + 3Qtz = Pet	+1.23	0.0
(Qtz, Spd)	4Ecr + 3PFO_2 = 3Amb + Pet	+7.92	+0.4
(Ecr, Spd)	Pet + PFO_2 = Amb + 4Qtz	+1.00	+1.0

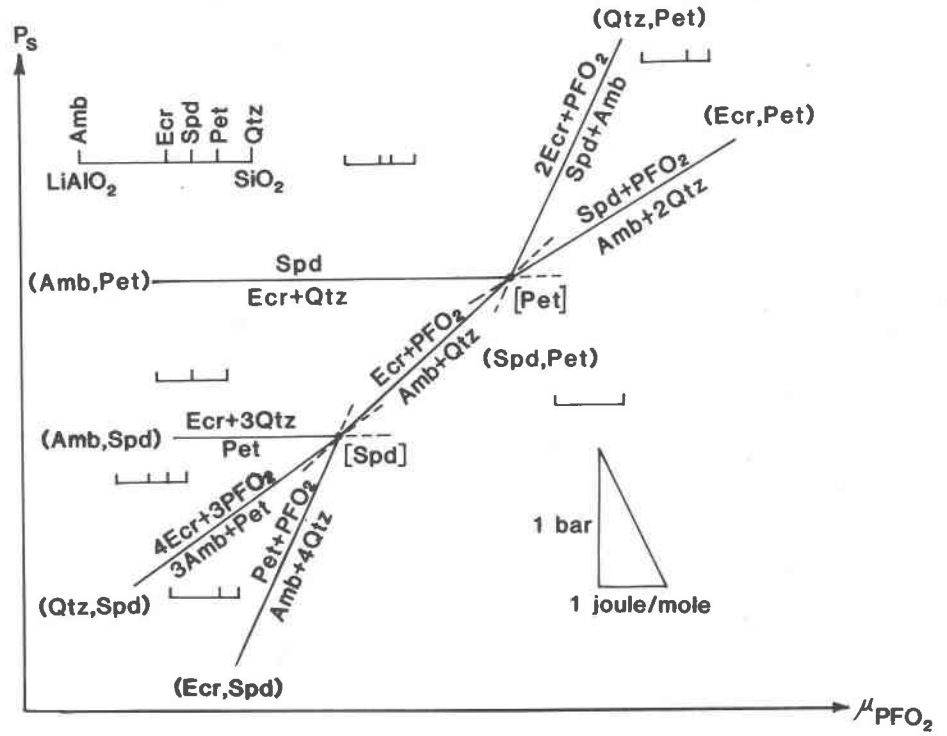

Fig. 10. Schematic isothermal P_s–μ_{PFO2} phase diagram in the system $LiAlO_2$–SiO_2–PFO_2, constructed from reactions listed in Table 6. This diagram is drawn for temperatures below the invariant point [BSP] in the lithium aluminosilicate phase diagram (London and Burt, 1982, Figure 4).

Finally, assemblages containing topaz, lepidolite, and quartz are common in gem-bearing pockets from highly differentiated pegmatites and form in KF-rich and HF-rich environments outside of the lithium aluminosilicate stability region.

Lithium aluminosilicate stabilities in granitic rocks

Spodumene and petalite occasionally occur as rare accessory minerals in leucogranites and aplites (*e.g.*, McLintock, 1923; Smithson, 1932; Lyakhovich, 1963; Chang, 1974), but lithium aluminosilicates generally are absent from Li-rich metasomatized granites (apogranites: Ginzburg and Lugovskii, 1977), in which the principal Li-bearing phases are amblygonite-montebrasite, lepidolite, and zinnwaldite. The proposed instability of spodumene at low pressures (London and Burt, 1982) probably limits its occurrence in these near surface environments, and all of the lithium aluminosilicates exhibit a susceptibility to metasomatic replacement. In H-, K-, and F-rich environments characteristic of greisenized granites, the lithium aluminosilicates become unstable with respect to muscovite, lepidolite, cookeite, kaolinite, and/or topaz. All of the lithium aluminosilicates may be replaced by albite in quartz-saturated, Na-rich environments (Figs. 4 and 5), and the fact that albite + amblygonite-montebrasite + quartz assemblages form outside of the lithium aluminosilicate stability region (Fig. 11) accounts for the absence of lithium aluminosilicates from Na-, P-, and F-rich granites containing this assemblage (*e.g.*, Lyakhovich, 1963; Exley and Stone, 1964; Aubert, 1969; Stone and George, 1978). The rarity of lithium aluminosilicates in granitic rocks emphasizes the well known (empirical) fact that in general, only pegmatitic processes are effective at concentrating lithium in sufficient quantities (relative to Na, K, P, F, *etc.*) to stabilize the lithium aluminosilicates.

Economic significance

The various factors that control lithium aluminosilicate stabilities in pegmatites and granites also may figure prominently in the crystallization of Cs, Rb, Nb, Ta, and Sn ore minerals. Deposits of columbite-tantalite, microlite-pyrochlore, and cassiterite commonly occur in albitized and greisenized portions of pegmatites, especially lithium-rich peg-

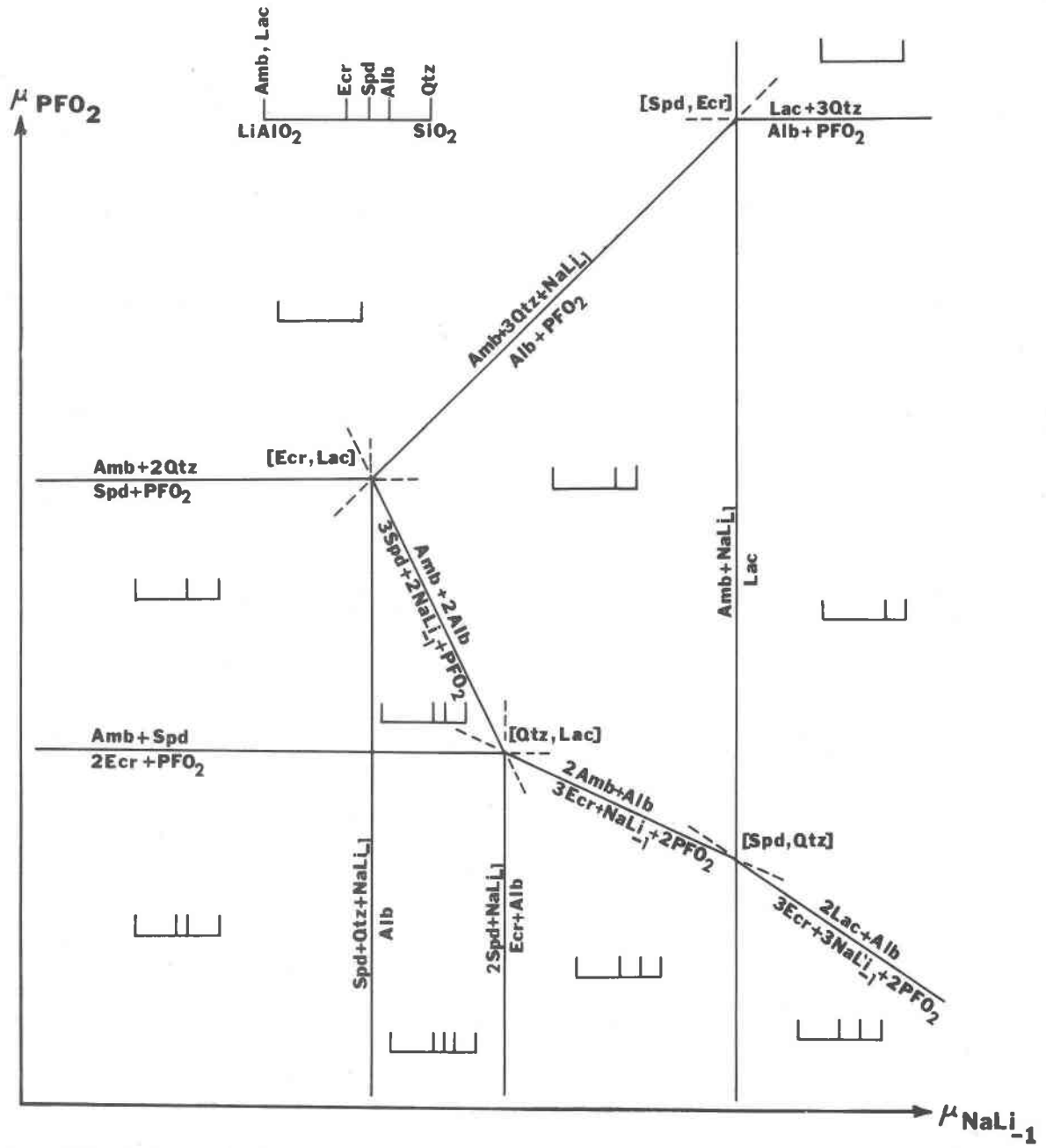

Fig. 11. Schematic isobaric-isothermal μ_{PFO2}–μ_{NaLi-1} phase diagram in the system $LiAlO_2$–SiO_2–PFO_2–$NaLi_{-1}$, constructed from reactions in Table 7 at temperatures sufficiently low that petalite is unstable. Eventual alteration of eucryptite to nepheline would occur to the lower right (not shown).

matites (*e.g.*, Vlasov, 1961, 1966; Ginzburg and Fel'dman, 1977; Ginzburg and Lugovskii, 1977). The micas themselves may be enriched in Cs and Rb (Rinaldi *et al.*, 1972).

The relationship between metasomatic alteration of spodumene and precipitation of rare-metal minerals is particularly evident at the Harding pegmatite, New Mexico. Studies by Jahns and Ewing (1976, 1977) point out that microlite is concentrated in masses of fine-grained Li-muscovite that replace microcline-spodumene pegmatite in the "spotted rock" zone. Additional work by Chakoumakos (1978a, 1978b) and by us has detailed numerous examples in which columbite or microlite is concen-

Table 7. Some univariant reactions in the system $LiAlO_2$–SiO_2–$NaLi_{-1}$–PFO_2 (Fig. 11)

Reactions	$(\delta\mu_{PFO_2}/\delta\mu_{NaLi_{-1}})_{P,T}$
$Alb + PFO_2 = Lac + 3Qtz$	0
$Spd + PFO_2 = Amb + 2Qtz$	0
$2Ecr + PFO_2 = Amb + Spd$	0
$Spd + Qtz + NaLi_{-1} = Alb$	∞
$2Spd + NaLi_{-1} = Ecr + Alb$	∞
$Amb + NaLi_{-1} = Lac$	∞
$Amb + 3Qtz + NaLi_{-1} = Alb + PFO_2$	+1
$3Ecr + 3NaLi_{-1} + 2PFO_2 = 2Lac + Alb$	-3/2
$3Ecr + NaLi_{-1} + 2PFO_2 = 2Amb + Alb$	-1/2
$3Spd + 2NaLi_{-1} + PFO_2 = Amb + 2Alb$	-2

trated at the borders of and within albite pseudomorphs of spodumene (Fig. 12).

These occurrences imply that in some cases, the precipitation of Nb-Ta minerals is paragenetically tied to the replacement of spodumene by albite (and muscovite or eucryptite). The replacement features seem to indicate that Na ⇌ Li or K ⇌ Li in spodumene involved the breakdown of alkali-rare metal–fluorine complexes. The relation clearly warrants further investigation, inasmuch as the occurrence of altered lithium aluminosilicates may potentially indicate the presence of rare-metal ores.

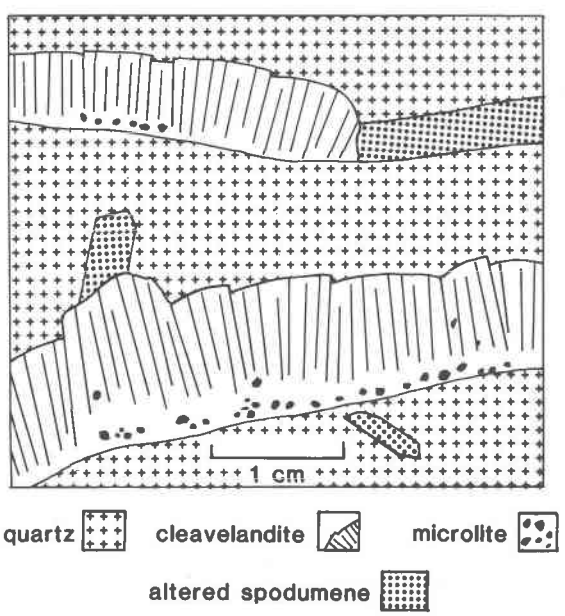

Fig. 12. Schematic cross section of cleavelandite pseudomorphs after spodumene from the Harding pegmatite, Taos County, New Mexico. Cleavelandite plates are roughly perpendicular to [001] of the original spodumene. Millimeter-size microlite crystals are segregated along the base of each pseudomorph. Small spodumene crystals are highly altered. Quartz adjacent to the microlite is smoky. University of New Mexico specimen #P11.3 (redrawn from Chakoumakos. 1978b, by permission of the author).

Acknowledgments

Carl A. Francis, Harvard University, Horace Winchell, Yale University, and John S. White, Jr., Smithsonian Institution, provided us with samples of altered lithium aluminosilicates from numerous localities. David R. Veblen, Johns Hopkins University, contributed electron images and diffraction patterns of altered spodumene. Eric J Essene, John M. Ferry, John R. Holloway, John W. Larimer, and David R. Veblen provided constructive reviews of the manuscript. We thank Kathryn Gundersen for typing the final manuscript and Sue Selkirk for drafting the diagrams.

The work was mainly supported by National Science Foundation Grant #EAR-7814785 to Arizona State University, which support is gratefully acknowledged.

References

Aubert, G. (1969) Les coupoles granitiques de Montebras de d'Echassieres (Massif Central français) et la genèse de leur minéralisations en étain, lithium, tungstène, et béryllium. Memoirs du Bureau de Recherches Géologiques et Miniéres, 46.

Bennington, K. O., Stuve, J. M., and Ferrante, J. M. (1980) Thermodynamic properties of petalite (Li_2Al_2, Si_8O_{20}). U. S. Bureau of Mines, Reports of Investigations, 8451.

Beus, A. A. (1960) Geochemistry of Beryllium and Genetic Types of Beryllium Deposits. Akademii Nauk SSSR, Moscow (transl. Freeman, San Francisco, 1967).

Brush, G. J. and Dana, E. S. (1880) On the mineral locality at Branchville, Connecticut. Fourth paper. Spodumene and the results of its alteration. American Journal of Science, 118, 257–285.

Burt, D. M. (1974) Concepts of acidity and basicity in petrology—the exchange operator approach. (abstr.) Geological Society of America Abstracts with Programs, 6, 674–676.

Burt, D. M. (1977) Mineralogy and petrology of skarn deposits. Rendiconti della Società Italiana de Mineralogia e Petrologia, 33 (2), 859–873.

Burt, D. M. and London, D. (1978) Sodium-lithium ion exchange among pegmatitic silicates and phosphates—a chemical model. (abstr.) Geological Society of America Abstracts with Programs, 10, 375.

Burt, D. M., London, D., and Smith, M. R. (1977) Eucryptite from Arizona, and the lithium aluminosilicate phase diagram (abstr.) Geological Society of America Abstracts with Programs, 9, 917.

Cameron, E. N., Jahns, R. H., McNair, A. H., and Page, L. R. (1949) Internal structure of granitic pegmatites. Economic Geology Monograph 2.

Cameron, and others (1954) Pegmatite investigations, 1942–45, New England. U. S. Geological Survey Professional Paper 255.

Chakoumakos, B. C. (1978a) Replacement features in the Harding pegmatite, Taos County, New Mexico. (abstr.) New Mexico Academy of Sciences Bulletin, 18, 22.

Chakoumakos, B. C. (1978b) Microlite, the Harding pegmatite, Taos County, New Mexico. Bachelor's honors thesis, University of New Mexico, Albuquerque, New Mexico.

Chang, J.-P. (1974) Preliminary study of a spodumene pegmatite in China [in Chinese with English abstract]. Geochimica, 182–191 (not seen; extracted from Mineralogical Abstracts, 26, 75–2418, 1975).

Exley, C. S. and Stone, M. (1964) The granitic rocks of southwest England. University of Exeter, Department of Geology Publication 32.

Ginzburg, A. I. and Feld'man, L. G. (1977) Deposits of tantalum and niobium. In Smirnov, V. I., Ed., Ore Deposits of the USSR, vol. 3. Nedra Press, Moscow (transl. Pitman, San Francisco, 372–424, 1977).

Ginzburg, A. I. and Gushchina, N. S. (1954) Petalite from pegmatites of eastern Transbaikalia [in Russian]. Trudy Mineralogicheskogo Muzeya Akademii Nauk SSSR, 6, 71–85 (not seen; extracted from Chemical Abstracts, 51, #4223, 1957).

Ginzburg, A. I. and Lugovskii, G. P. (1977) Deposits of lithium. In Smirnov, V. I., Ed., Ore Deposits of the USSR, vol. 3. Nedra Press, Moscow (transl. Pitman, San Francisco, 295–311, 1977).

Graham, J. (1975) Some notes on α-spodumene, $LiAlSi_2O_6$. American Mineralogist, 60, 919–923.

Hanley, J. B., Heinrich, E. W., and Page, L. R. (1950) Pegmatite investigations in Colorado, Wyoming, and Utah. U. S. Geological Survey Professional Paper 227.

Jahns, R. H. (1946) Mica deposits of the Petaca district, Rio Arriba County, New Mexico. New Mexico Bureau of Mines and Minerals, Socorro, Bulletin 25.

Jahns, R. H. (1955) The study of pegmatites. Society of Economic Geologists, 50th Anniversary Volume, Part II, 1025–1130.

Jahns, R. H. and Burnham, C. W. (1969) Experimental studies of pegmatite genesis. I. A model for the derivation and crystallization of granitic pegmatites. Economic Geology, 64, 843–864.

Jahns, R. H. and Ewing, R. C. (1976) The Harding mine, Taos County, New Mexico. New Mexico Geological Society Guidebook, 27th Field Conf., Vermejo Park, 263–276.

Jahns, R. H. and Ewing, R. C. (1977) The Harding Mine, Taos County, New Mexico. Mineralogical Record, 8, 115–126.

Jenks, W. F. (1935) Pegmatites at Collins Hill, Portland, Connecticut. American Journal of Science 230, 117–197.

Jones, R. W., Jr. (1964) Collecting fluorescent minerals. Rocks and Minerals, 7–8, 399.

Julien, A. A. (1879) On spodumene and its alterations from the granite-veins of Hampshire County, Massachusetts. Annals of the New York Academy of Science, 1, 318–359.

Korzhinskii, D. S. (1957) Physicochemical Basis of the Analysis of the Paragenesis of Minerals. Izvestiya Akademii Nauk SSSR, Moscow (transl. Consultants Bureau, New York, 1959).

Krygina, V. E. (1948) Spodumene from the Altyn-Tau deposits [in Russian]. Zapiski Vsesoyuznogo Mineralogischeskogo Obshchestva, 77, 320–322 (not seen; extracted from Chemical Abstracts, 44, #6355h, 1950).

Loh, S. E., and Wise, W. S. (1976) Synthesis and fluorine-hydroxyl exchange in the amblygonite series. Canadian Mineralogist, 14, 357–363.

London, D. (1979) Occurrence and Alteration of Primary Lithium Minerals, White Picacho Pegmatites, Arizona. Masters thesis, Arizona State University, Tempe, Arizona.

London, D. and Burt, D. M. (1979) Processes of formation and destruction of eucryptite in lithium pegmatites. (abstr.) Transactions of the American Geophysical Union, 60, 417.

London, D. and Burt, D. M. (1980) Local lowering of silica activity during albitization of spodumene—its relation to the formation of micas and eucryptite. (abstr.) Transactions of the American Geophysical Union, 61, 404.

London, D. and Burt, D. M. (1982) Lithium aluminosilicate occurrences in pegmatites and the lithium aluminosilicate phase diagram. American Mineralogist, 67, 483–493.

Lyakhovich, V. V. (1963) Petrographic and mineralogical features of granites containing amblygonite and spodumene. Izvestiya Akademii Nauk SSSR, Seriya Geolgicheskaya, 3, 63–83 (transl. International Geology Review, 7, 157–169).

McLaughlin, T. G. (1940) Pegmatite dikes of the Bridger Mountains, Wyoming. American Mineralogist, 25, 46–48.

McLintock, W. F. P. (1923) On the occurrence of petalite and pneumatolytic apatite in the Meldon aplite, Okehampton, Devonshire, England. Mineralogical Magazine, 20, 140.

Mrose, M. E. (1953) The α-eucryptite problem. (abstr.) American Mineralogist, 38, 353.

Mrose, M. E. (1971) Lacroixite: its redefinition and new occurrences. (abstr.) 20th Clay Minerals Conference, 8th Annual Meeting of the Clay Minerals Society with the Mineralogical Society of America, Abstracts with Programs, 10.

Munoz, J. L. (1971) Hydrothermal stability relations of synthetic lepidolite. American Mineralogist, 56, 2069–2087.

Nazarova, A. S. (1961) Two generations of spodumene from pegmatites [in Russian with English summary]. L'vovskii Mineralogischeskogo Sbornik, 15, 182–188.

Nel, H. J. (1946) Petalite and amblygonite from Karibib, Southwest Africa. American Mineralogist, 31, 51–57.

Page, L. R. and others (1953) Pegmatite investigations, 1942–45, Black Hills, South Dakota. U. S. Geological Survey Professional Paper 247.

Parga-Pondal I., and Cardoso, G. M. (1948) Die Lithium-pegmatit von Lalin in Galizien (prov. Pontevedra, Spanien). Schweizerische Mineralogische und Petrographische Mitteilungen, 28, 324–334.

Quensel, P. (1937) Minerals of the Varaträsk pegmatite. IV. Petalite and its alteration product, montmorillonite. Geologiska Föreningen i Stockholm Förhandlingar, 59, 150–156.

Quensel, P. (1938) Minerals of the Varuträsk pegmatite. X. Spodumene and its alteration products. Geologiska Föreningen i Stockholm Förhandlingar, 60, 201–215.

Rao, A. B. (1962) On pseudomorphs of spodumene from Borborrema pegmatites. Annals of the Academy of Brazilian Science, 34, 455–463 (not seen; extracted from Mineralogical Abstracts, 16 (5), 489, 1964).

Rinaldi, R. Černý, P. and Ferguson, R. B. (1972) Lithium–rubidium–cesium micas. Canadian Mineralogist, 11, 690–707.

Robie, R. A., Hemingway, B. S., and Fisher, J. R. (1978) Thermodynamic properties of minerals and related substances at 298.15 K and 1 bar (10^5 Pascals) pressure and at higher temperatures. U. S. Geological Survey Bulletin 1452.

Rossovskii, L. N. and Klochkova, G. N. (1965) Discovery of petalite–microcline pegmatites [in Russian]. Zapiski Vsesoyuznogo Mineralogicheskogo Obshchestva, 94, 507–515 (not seen; extracted from Mineralogical Abstracts, 17, 691–692, 1966).

Saito, N. Kokubu, N., and Kakihana, H. (1950) Alteration of petalite. Journal of the Chemical Society of Japan, Pure Chemistry Section, 71, 131–133.

Sakurai, K., Bunno, M., Masahiro, A., and Yasumitsu, S. (1977) Some minerals in lithium pegmatite from Myokenzan, Ibaraki Prefecture, Japan (in Japanese). Gaseki-kobutsu-kosho Gakkaish, 72, 13–27.

Schwartz, G. M. (1937) Alteration of spodumene to kaolinite in the Etta mine. American Journal of Science, 233, 303–307.

Schwartz, G. M. and Leonard, R. J. (1926) Altered spodumene from the Etta mine, South Dakota. American Journal of Science, 211, 257–264.

Shainin, V. E. (1946) The Branchville, Connecticut, pegmatite. American Mineralogist, 31, 329–345.

Shibata, H. (1952) Spodumene and amblygonite from the Bunsen mine, and other localities in Korea. Scientific Reports of the Tokyo Bunrika Daigaku, Section C, 2 (11), 145–153.

Smithson, F. (1932) The petrography of the northern portion of the Leinster granite. Geological Magazine, 69, 465–474.

Sosedko, A. F. (1964) Muscovite-oligoclase pseudomorphs after spodumene [in Russian]. Mineralogiya i Geokhimiya, Leningradskii Gosudarstvennii Universitet, 1, 57–61 (not seen; extracted from Chemical Abstracts, 62, #12909f, 1965).

Sosedko, A. F. and Gordienko, V. V. (1957) Eucryptite from the pegmatite of the northern part of the Kola Peninsula. Doklady Akademii Nauk SSSR, 116, 135–136 (transl. Doklady of the Academy of Sciences, USSR, Earth Science Sections, 116, 873–875, 1957).

Stewart, D. B. (1963) Petrogenesis and mineral assemblages of lithium-rich pegmatites. (abstr.) Geological Society of American Special Paper 76, 159.

Stewart, D. B. (1978) Petrogenesis of lithium-rich pegmatites. American Mineralogist, 63, 970–980.

Stone, M. and George, M. C. (1978) Amblygonite in leucogranites of the Tregonning-Godolphin granite, Cornwall. Mineralogical Magazine, 42, 151–152.

Sundelius, H. W. (1963) The Peg Claims spodumene pegmatites, Maine. Economic Geology, 58, 84–106.

Thompson, J. B., Jr. (1955) The thermodynamic basis for the mineral facies concept. American Journal of Science, 253, 65–103.

Tien, T. Y. and Hummel, F. A. (1964) Studies in lithium oxide systems: XIII. $Li_2O{\cdot}Al_2O_3{\cdot}2SiO_2$–$Li_2O{\cdot}Al_2O_3{\cdot}GeO_2$. Journal of the American Ceramic Society, 47, 582–584.

Varlamoff, N. (1960, 1961) Matériaux pour l'étude des pegmatites du Congo Belge et du Ruanda. Quatrième note: Pegmatites à amblygonite et à spodumène et pegmatites fortement albitiées à spodumène et à cassitérite de la région de Katumba (Ruanda). Annales de la Société Géologique de Belgique, 84, 257–278 (not seen; extracted from Mineralogical Abstracts, 15, 393, 1962).

Vlasov, K. A. (1961) Principles of classifying granite pegmatites and their textural-paragenetic types. Izvestiya Akademii Nauk SSSR, Seriya Geologischeskaya, 1, 5–20 (transl. Izvestiya of the Academy of Sciences, USSR, Geological Series, 1, 5–20, 1961).

Vlasov, K. A. (1964–66) Geochemistry and Mineralogy of Rare Elements and Genetic Types of Their Deposits (3 vols.) Nauka Press, Moscow (transl. Israel Program for Scientific Studies, Jerusalem, 1966–1968).

Manuscript received, April 6, 1981;
accepted for publication, January 11, 1982.